Sonja Kristiansson

UV Light Bonding in Manufacturing of Transparent Displays

Metropolia University of Applied Sciences

Bachelor of Engineering

Biotechnology and Chemical Engineering

Bachelor's Thesis

7 March 2023

Abstract

Author:	Sonja Kristiansson
Title:	UV Light Bonding in Manufacturing of Transparent Displays
Number of Pages:	38 pages + 4 appendices
Date:	7 March 2023
Degree:	Bachelor of Engineering
Degree Programme:	Biotechnology and Chemical Engineering
Professional Major:	Chemical Engineering
Supervisors:	Azad Karis, Process Development Manager Kai Laitinen, Principal Lecturer

The goal for this thesis was to research the capability of the new bonding process for attaching the electroluminescent display (ELD) and the flexible printed circuit (FPC) together as well as to optimize the bonding process parameters. Process is executed with UV light bonder machine using a conductive UV light cured adhesive. This project was done for Lumineq Oy, which is specialized in manufacturing transparent displays using a thin film electroluminescent display technology.

Experimental part of this thesis consisted of tests, which were designed to research suitable parameters for the new bonding process. Design of experiment (DOE) was executed following a full factorial design 3^3. Conductive particle concentration, force of the bonding blade and UV light curing time were selected as factors on the basis of their impact on the most important properties of bonding process: conductivity, adhesion, and mechanical strength of the bond line.

Samples were visually inspected, and functionality was tested by connecting samples to power and straining them in high temperatures. The factors did not show any major impact to functionality, due to full function of the displays in all samples, including temperature effect. The conductivity of the bond line was evaluated with resistance measurements, and a tensile strength test was performed to evaluate the strength of the bond line. DOE with results were analysed using general factorial regression test. Model results showed that force as a single factor and particle concentration combined with force have the most impact on resistance and therefore the conductivity. Higher forces led to lower resistance values. Particle concentration had the largest impact on strength. Lower concentrations in the adhesive led to higher strength on the bond line.

The experiment provided information about the capability of UV light bonding process and the behaviour of the parameters. The process is feasible, reliable, and scalable based on this initial experiment and research. More research should be conducted to determine the process limits for parameters and to specify the process window. In addition, more research is required to obtain more data about the process behaviour.

Keywords: ACF, photopolymerisation, UV light bonding, DOE

Tiivistelmä

Tekijä:	Sonja Kristiansson
Otsikko:	UV-valobondaus läpinäkyvien näyttöjen valmistuksessa
Sivumäärä:	38 sivua + 4 liitettä
Aika:	7.3.2023

Tutkinto:	Insinööri (AMK)
Tutkinto-ohjelma:	Bio- ja kemiantekniikka
Ammatillinen pääaine:	Kemian prosessitekniikka
Ohjaajat:	Prosessikehityspäällikkö Azad Karis Yliopettaja Kai Laitinen

Insinöörityön tavoite oli tutkia uuden bondausprosessin kyvykkyyttä elektroluminesenssinäytön ja joustavan piirilevyn liittämiseksi (bondaus) sekä optimoida prosessin parametrit. Prosessi toteutetaan UV-valokäyttöisellä bondauslaitteella käyttäen sähkönjohtavaa UV-valolla kovetettavaa liimaa. Tämä työ toteutettiin Lumineq Oy:lle, joka on erikoistunut läpinäkyvien näyttöjen valmistamiseen ohutkalvoelektroluminesenssiteknologialla.

Työn kokeellinen osuus koostui testeistä, joiden perusteella selvitettiin sopivia parametreja bondausprosessille. Koesuunnitelma toteutettiin käyttäen täydellistä faktorisuunnitelmaa 3^3, johon valittiin muuttujiksi sähkönjohtavien partikkelien konsentraatio, bondausterän aiheuttama voima ja UV-valon kovetusaika bondausprosessin tärkeimpien ominaisuuksien (johtavuus, adheesio ja mekaaninen lujuus) perusteella.

Testinäytteet tutkittiin visuaalisesti ja toimivuutta testattiin kytkemällä näyttöihin virta ja kuormittamalla niitä korkeassa lämpötilassa. Näyttöjen toiminnallisuus säilyi, jopa lämpötilan kuormituksen jälkeen. Liitoksen sähkönjohtavuutta arvioitiin resistanssimittauksilla ja adheesiota ja lujuutta varten suoritettiin vetolujuustesti. Tulokset yhdessä koesuunnitelman kanssa analysoitiin käyttäen regressioanalyysia. Mallin tulokset osoittivat voimalla yksittäisenä muuttujana ja voiman sekä partikkelikonsentraation yhteisvaikutuksella olevan merkittävin vaikutus resistanssiin. Korkeammat voiman arvot johtivat matalampaan resistanssiin. Myös partikkelikonsentraatiolla oli suurin vaikutus lujuuteen. Matalammat konsentraatiot liimassa johtivat korkeampaan lujuuteen liitoksessa.

Työ tarjosi tietoa UV-valokäyttöisen bondausprosessin kyvykkyydestä sekä parametrien käyttäytymisestä. Tutkimuksen perusteella prosessi on toteuttamiskelpoinen, luotettava sekä skaalattavissa. Lisätutkimuksia tarvitaan prosessin rajojen ja prosessi-ikkunan selvittämiseksi sekä lisätiedon saamiseksi prosessin käyttäytymisestä.

Avainsanat: ACF, fotopolymerisaatio, UV-valobondaus, DOE

Contents

Appendices

List of Abbreviations

ACA: Anisotropically conductive adhesive

ACF: Anisotropic conductive film

Ag: Silver

Au: Gold

BiSn: Bismuth-tin alloy

DOE: Design of Experiment

ECA: Electrically conductive adhesive

ELD: Electroluminescent display

FPC: Flexible printed circuit

HUD: Heads-up-display

ICA: Isotropically conductive adhesive

IC: Integrated circuit

IEC: International Electrotechnical Commission

ITO: Indium tin oxide

LCD: Liquid crystal display

LED: Light emitting diode

MTBF: Mean Time Between Failure

mW/cm^2:	milliwatt/square centimetre
μm:	Micrometre
N:	Newton
Ni:	Nickel
nm:	Nanometre
Ohm:	Resistance (Ω)
OLED:	Organic light emitting diode display
PDP:	Plasma display panel
sec:	Second
SnAg:	Tin-silver alloy
SnAgCu:	Tin-silver-copper alloy
SnCu:	Tin-copper alloy
SnPb:	Tin-lead
SnZn:	Tin-zinc alloy
TAB:	Tape automated bonding
UV:	Ultraviolet
UV-A:	Ultraviolet radiation with a range of 315–400 nanometres.
UV-B:	Ultraviolet radiation with a range of 280-315 nanometres.

UV-C: Ultraviolet radiation with a range of 100-280 nanometres.

vol%: Volume percent

wt%: Weight percent

1 Introduction

Bonding is a process for joining various elements together. It is used to viewpoint of assembly to form products such as packaging, equipment spare parts, or any kind of elements that need to be attached together. Conductivity is required from the bonding process, for example in the case of electronic devices that require electrical connection. Different surfaces need interconnect materials between them to form adhesion. In addition, physical quantities are applied to the process to support the joining process and wanted properties.

The research of this thesis was executed for Lumineq Oy located in Espoo. Lumineq Oy is a global market leader for transparent displays using a thin film electroluminescent display technology. Lumineq provides heads-up-displays (HUDs) and in-glass integrated displays for various applications such as optical devices and vehicles. The goal for this thesis is to research the capability of new bonding process for attaching the electroluminescent display (ELD) and the flexible printed circuit (FPC) together as well as to optimize the bonding process parameters. The new process is executed with a UV light bonder machine using a conductive UV light cured adhesive. The current process utilises an anisotropic conductive film (ACF) with manual execution. The new process will establish automation in the bonding process, resulting in faster lead time and minimizing development of rejects. UV light cured adhesive provides higher adhesion and better resistant to moisture. These will result in higher quality and yield.

Thesis includes a general introduction to the bonding process and interconnect materials, focusing mainly on the bonding process between FPC and ELD. Bonding using ACF and UV light cured adhesive is also addressed, including an introduction to chemistry behind the cure. The experimental part consists of tests executed and optimized following a design of experiment. Samples are visually inspected and connected to power to test functionality. Temperature and strength test along with resistance measurements are also implemented to research the reliability, capabilities, and properties of the process.

2 Bonding of FPC and ELD

Bonding stands for the attachment process of two or multiple parts. Parts of same or different materials are joined together permanently. Bonding processes vary depending on the joining mechanism. For example, in the adhesive bonding process, the adhesive material is applied to parts surfaces. After curing, the adhesive substance creates bonds between the parts, joining them together permanently. [1.]

The field of electronic product manufacture widens the definition of bonding. Electronic components are connected to power distribution in the bonding process. Developing a functional electronic device, driver integrated circuits (ICs) and electronic components are physically integrated together with interconnect materials. [2, p. 1.] This electrical interconnection can be achieved by various bonding techniques, for example, flip-chip bonding, wire bonding and tape automated bonding (TAB) [3, p. 26].

Corresponding conductive surfaces (pads) of IC and the device (substrate) are aligned with each other, leaving insulation gaps between pads. Simplified illustration of the bonding process is presented in Figure 1 and Figure 2. IC can be a form of microchip or flexible printed circuit (FPC). Interconnect material is applied between surfaces to attach components together. [4, p. 14; 5, p. 41; 6, p. 26-27.] Depending on the material, substances require different conditions to cure [2]. Typically, pressure load and/or heat are applied to establish strong adhesion and contact between surfaces [4, p. 14; 5, p. 41; 6, p. 26-27].

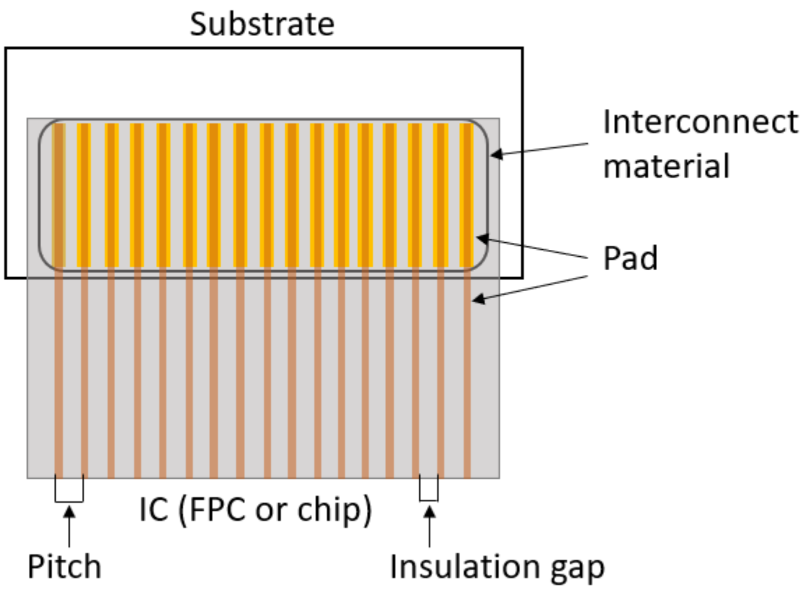

Figure 1. Schematic illustration (top view) of the bonding process with IC and substrate pad alignment [7].

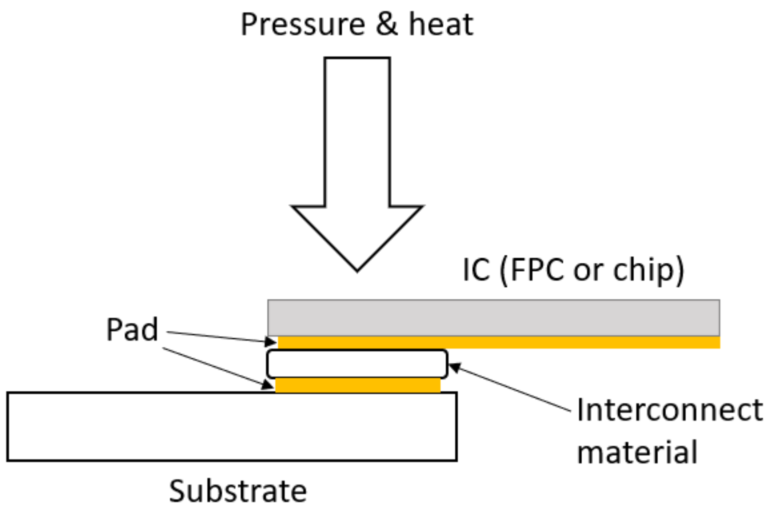

Figure 2. Schematic illustration (side view) of the bonding process [7].

2.1 Interconnect materials

Interconnect materials are used to make electrical conductivity between ICs and the substrate's attachment surfaces possible. Materials also provide adhesion and mechanical strength in the interface of joined surfaces. Variety of different interconnect materials are being used. They can be lead-containing solder alloys such as tin-lead (SnPb) or lead-free solders such as tin-silver alloy (SnAg), tin-copper alloy (SnCu), tin-silver-copper alloy (SnAgCu), tin-zinc alloy (SnZn) and bismuth-tin alloy (BiSn). [2, p. 11, 14.]

Electrically conductive adhesives (ECAs) are another option for lead-free interconnect materials. ECAs are mostly composed of organic/polymeric binder and conductive fillers such as metallic particles or polymer spheres with a metallic coating. [2, p. 15, 227.] Metallic fillers act as conductors providing electrical conductivity. The fillers come in different sizes and shapes depending on the type of ECA. Polymeric binders join components to each other providing adhesion and mechanical strength and act as an insulator. ECAs can be divided into two types of conductive adhesives: isotropically conductive adhesives (ICAs) and anisotropically conductive adhesives (ACAs). [2, p. 15.]

ICAs commonly contain 1-10 µm sized silver (Ag) flakes and provide electrical conductivity in the direction of all x, y, and z axes, due to larger filler concentration approximately 25-30 vol% [2, p. 17; 8]. Conventional ACAs contain adhesive resin with dispersed conductive metallic particles, which can be made of gold (Au), silver or nickel (Ni). Particles can also be polymer balls with metallic coating. Anisotropic conductive films (ACFs) can be classified in the same category as ACAs due to the same composition. The only major difference is that the ACA comes in the form of a liquid adhesive, and ACF in the form of a film. [4, p. 14-15.] ACAs typically contain 3-5 µm sized rounded metal particles and have an electrical conductivity only in the direction of z axis, due to smaller filler concentration approximately 5-10 vol% [2, p. 15, 17, 227; 8].

ACAs and ACFs are widely used as lead-free interconnect materials in the bonding process of electronic products, due to their technical advantage. Both are suitable options for ultra-fine pitch applications compared to solder alloys. They provide electrical interconnection in shorter pad spacing as narrow as 40 µm. [9; 10.] They are also more affordable, withstand harsh conditions as well as are environment friendly [9].

ACAs and ACFs are utilized as interconnect material in various bonding processes specially in the field of Flat Panel Display technology including electroluminescent displays (ELD), liquid crystal displays (LCD), plasma display panels (PDP) and organic light emitting diode displays (OLED) [2, p. 231; 11].

2.2 Bonding techniques

2.2.1 ACF bonding

ACF is an adhesive film with randomly dispersed conductive particles [4].
Typically, conductive particles are metal-coated polymer spheres [9, p. 226]. General use of ACF is to develop an electrical interconnection between tin coated copper pads of IC and indium tin oxide (ITO) electrodes of glass substrate [12, p. 775; 9, p. 226].

Important parameters for bonding process with ACF are pressure load, temperature and curing time. Heat and pressure are applied simultaneously to attach IC on the substrate. [2, p. 230.]

ACF’s polymer resin requires specific temperature to cure. The curing degree has an impact on mechanical properties of ACF such as strength. Generally, longer curing times at the selected temperature produce higher curing degrees. The applied heat will soften ACF and allows it to flow and position particles evenly. [13; 14, p. 1186.] Polymer cures forming a crosslinked three-dimensional polymer networks. This will lead to a rapid phase change. Soft structure of the film changes into solid. [4, p. 15.] Polymerisation reaction can occur through either a step-growth route or a chain-growth route. The route of the reaction depends on the type of curing agent in the resin. Network structure hardens ACF and joins components together permanently, providing bond mechanical strength. [14, p. 1186.]

Electrical path is established by trapping conductive particles between pads of the IC and the substrate [9, p. 226]. Simplified illustration of the bonding process with ACF is presented in Figure 3. To create the path, particles and pads must have mechanical contact with each other. This could be achieved by applying pressure during the bonding process. Pressure deforms conductive particles creating conduction joints between them and the corresponding pads. [15.]

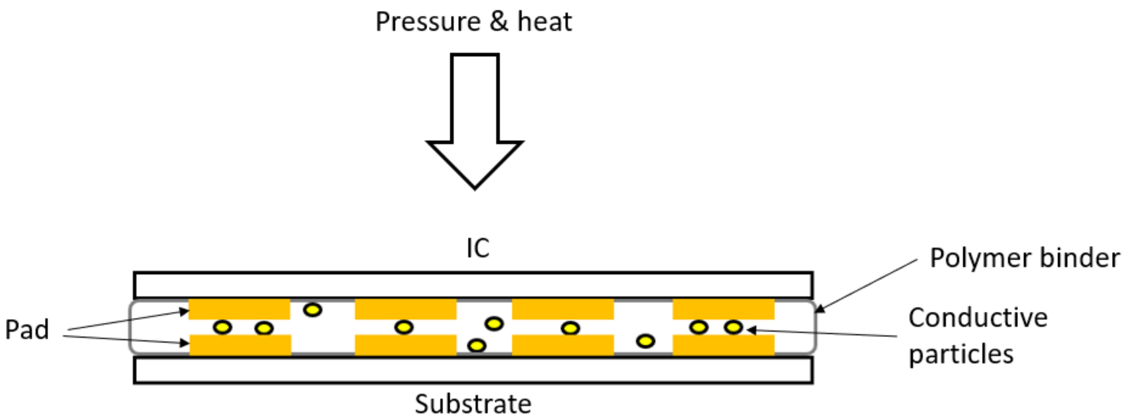

Figure 3. Schematic illustration (cross-section side view) of the ACF bonding process [2, p. 231].

The force of the pressure affects the deformation of particles, which changes performance of ACF's electrical interconnects. In an ideal situation, the particle's contact area between surfaces should be at the largest when particles squash before breaks occur in the metallic layers. Too much pressure will tear the particle's metallic coating exposing the polymer filling, which will lead to failure in the electrical conductivity between IC and the substrate. To obtain conductivity only in the vertical direction, particles must not be in contact with each other, otherwise it may result a short circuit. Short circuit can be prevented by controlling pressure, particle size and concentration of the film. [15.]

2.2.2 UV light bonding

Ultraviolet (UV) light is a short wavelength from 100 nm to 400 nm [16]. UV radiation spectrum is presented in Figure 4. There are three ranges in UV radiation spectrum: UV-C (100-280 nm), UV-B (280-315 nm) and UV-A (315-400 nm). [16; 17, p. 6.] UV-A light contains the least amount of energy, which makes it the least harmful and most common type of UV light. It has the ability to cause fluorescent materials to emit visible light, which is commonly used in tanning booths and UV-A lamps. UV-B is considered to be the most harmful type of UV light and it is known to cause skin cancer. UV-C light absorbs almost completely in the air in nature and has the ability to kill bacteria. UV-C lamps are used to purify air and water. [17, p. 6.]

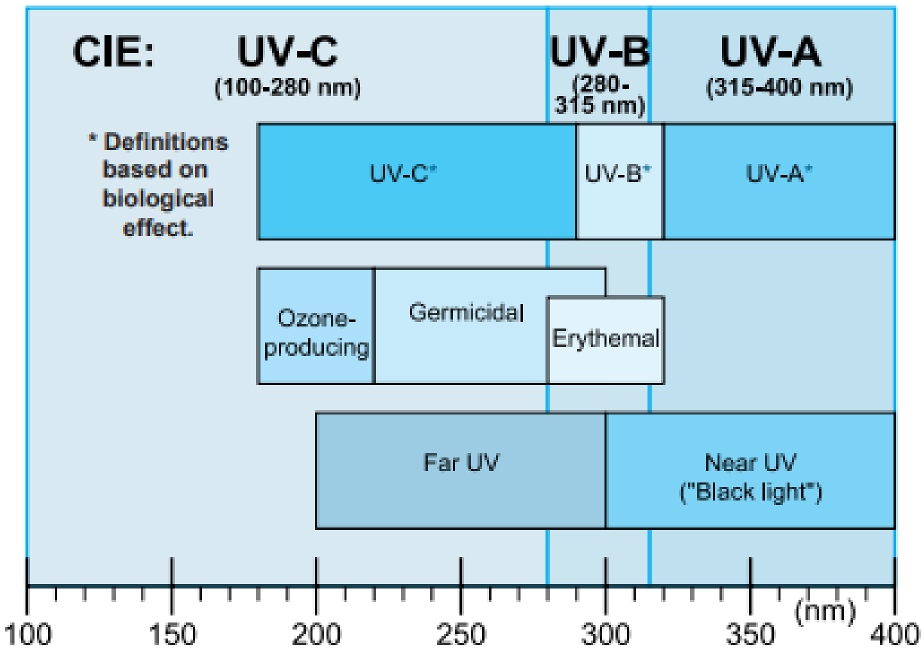

Figure 4. UV radiation spectrum [17, p. 6].

UV radiation is widely used in dental, medical, and industrial processes [18]. Hardening of a liquid substance with applied UV light, is called UV radiation curing [19]. The method has been utilized for curing coatings, inks, paints, varnishes, and adhesives in various industrial applications [20, p. 15; 21]. Composition of the substance varies depending on the application. Base composition contains polymers, photoinitiators and non-solvent diluents. [19.] Curing begins when the substance is exposed to UV radiation. UV light initiates a polymerisation reaction, which results to rapid phase change. The liquid substance phase changes into solid after curing. [21.]

UV radiation curing is a suitable option in bonding processes. Adhesive act as a connect material between joined surfaces. Once adhesive is cured, it provides adhesion and mechanical strength in the interface of attached components. Multiple bonding processes utilizing UV light cured adhesives require UV light penetration through the bond line. At least one of the attached components should be clear or translucent, which makes UV radiation curing suitable for bonding glass to glass or glass to other materials. However, thermal expansion of different materials must be taken into consideration to avoid high stresses. [22, p. 406.]

There are a wide range of UV light cured adhesives available in industrial applications and some guidelines to follow. Most of the adhesives are cured by the free-radical or cationic polymerisation mechanism. In the reaction, polymer chains in the adhesive form a crosslinked network structure. This will lead to a phase change of the liquid adhesive to solid. [22, p. 406.]

The process requires correct wavelength and UV light intensity to achieve an optimum cure. The majority of adhesives are cured in the UV-A wavelength of 365 nm. Some adhesives might require curing in the visible end of UV radiation spectrum, wavelengths 400-450 nm. Curing is the result of the polymerisation reaction, which is initiated by UV light. The applied UV light activates the initiator in the adhesive. The UV light source should be selected from the UV radiation spectrum, to match with the initiator in the adhesive. [22, p. 406.]

The intensity of UV light is expressed using units of mW/cm^2. Low intensity is considered to be 5-10 mW/cm^2 and high intensity 100-1000 mW/cm^2. Curing time will depend on the UV light intensity. Higher intensity's require shorter curing times. [22, p. 406-408.] Medium pressure mercury UV lamps or electrodeless UV lamps are currently commonly used as light sources. Light emitting diode (LED) lamps can be used in smaller spaces, and they prevent the generation of large amount of heat during curing process. [19.]

Secondary cure might be required in applications, where it is not possible to expose the entire adhesive to the UV radiation. After applied UV light, curing of the adhesive will be completed in the secondary cure process. Options for secondary cure are shadow curing and adding heat or moisture to the process. Anaerobic adhesives will continue to cure in the shadows after the UV light is removed and in the absence of oxygen. Adhesives that contain silicone and cyanoacrylates continue to cure in the presence of atmospheric moisture or surface moisture. [22, p. 407.]

3 Polymerisation

Monomers are smallest and simplest forms of molecules in organic chemistry. All monomers have the capacity to react with other monomers or molecules and form chemical bonds to yield larger molecules, oligomer or polymer. [23, p. 5.] Polymers are large molecules containing repeating units of monomers which are connected by covalent bonds [24, p. 363; 25, p. 2]. Oligomers are composed of few monomers [26]. Polymerisation is chemical reaction between hydrocarbon molecules, where molecules join together by covalent bonds yielding a polymer [24, p. 363]. Polymerisation reaction is divided into two main groups, step-growth and chain-growth polymerisation, based on the reaction mechanism. Reactions can be divided further into subgroups based on the reaction route. [23, p. 5; 24, p. 363.]

3.1 Structures of polymers

Polymers have different molecular structures depending on how monomer units are connected [23, p. 7; 25, p. 2]. Simplified illustration of the structures is presented in Figure 5. The most simple polymer structure is the linear polymer. This polymer consists of repeating monomer units, which are connected to each other in a linear chain. [25, p. 2-3.] Monomers that have more than two reactive groups can form a branched or crosslinked network structure [24]. A branched structure is formed when single small branches attach to the main linear chain. Other forms of branched polymers are star- and comb-shaped structures. Crosslinked network structures are formed when polymer chains with branched structure interconnect together forming a large macromolecule. Networks can be planar or three-dimensional, which resembles the structure of diamonds. [23, p. 7-8; 25, p. 3.]

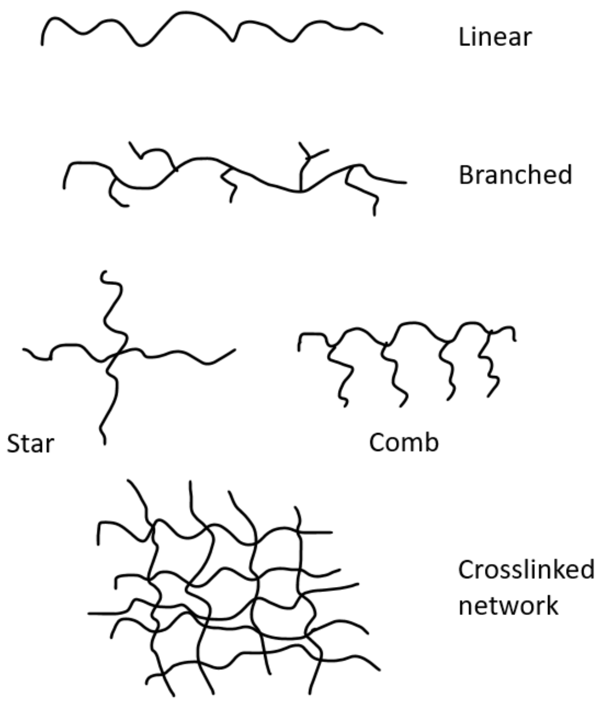

Figure 5. Schematic illustration of polymer structures [25, p. 3].

Polymer structures can contain either single repeating structural units or different units. Polymer structure that contains two or more different structural units is called copolymer, which can be linear or branched. [25, p. 3-4.]

3.2 Step-growth polymerisation

Step-growth polymerisation is also well-known as condensation polymerisation [23, p. 5]. Polymers are built by several consecutive condensation reactions, where small molecules such as water and alcohol are eliminated [23, p. 5; 24, p. 363]. In order to build a step-growth polymer, the reaction requires a monomer which contains at least two functional groups or two monomers with different molecular formula with equal molar amounts and two functional groups. The opposite ends of the monomer are both reactive, which enables reaction to proceed stepwise consecutively and rather spontaneously. [24, p. 363; 27, p. 59; 28.] The reaction occurs between any of the different sized molecules present in the reaction, and the polymer chain size doubles with each step. This is one of the major differences to chain-growth polymerisation. [29.] In addition, polymer formation occurs due to only one reaction stage. The reaction proceeds by individual reactions of the functional groups and can occur in any of the reactive ends. This will slowly increase the size of the polymer chain. [28.]

Simplified illustration of the reaction is presented in Figure 6. Two monomers react to form a dimer. The dimer continues to react with another dimer to yield a tetramer or can react with a monomer to yield a trimer. This process continues in each reaction at same relatively slow reaction rate until a large polymer is formed. [28.]

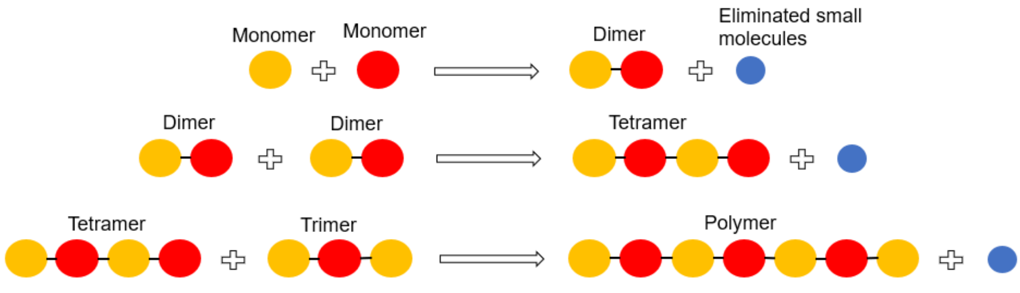

Figure 6. Schematic illustration of the step-growth polymerisation [28].

3.3 Chain-growth polymerisation

Chain-growth polymerisation is also well-known as addition polymerisation [23, p. 5]. Polymers are formed by several consecutive additions of monomer units with the same molecular formula containing carbon-carbon double bonds. Additions are radical or ionic chain reactions without elimination of any molecules. [24, p. 365.] Unlike spontaneous step-growth polymerisation, chain-growth polymerisation requires an initiator or a catalyst [27, p. 61]. Chain reaction involves typically at least three reaction stages: initiation, propagation, and termination [23, p. 5].

A simplified illustration of the reaction is presented in Figure 7. The reaction begins at the initiation stage; the initiator is used to produce an initiator species R* with a reactive centre. The initiator will react with an unreactive monomer, adding it to the reactive centre and convert it to a reactive intermediate. In the propagation stage, the activated monomer is now capable of reacting with another monomer, which is added to the chain. Added monomers react only with the reactive centre of the polymer chain, which will be regenerated after every added monomer. Successive additions to the reactive centre continue until the final termination stage, where the initiator will be deactivated. Compared to the step-growth polymerisation, polymer chain grows one monomer at a time and the additions are rapid, which makes the whole polymerisation much faster. [24, p. 365; 25; 29; 30.] There are three different types of initiator species; free radicals, anions, and cations. Polymerisation will follow different routes depending on the used initiator. [24, p. 365.]

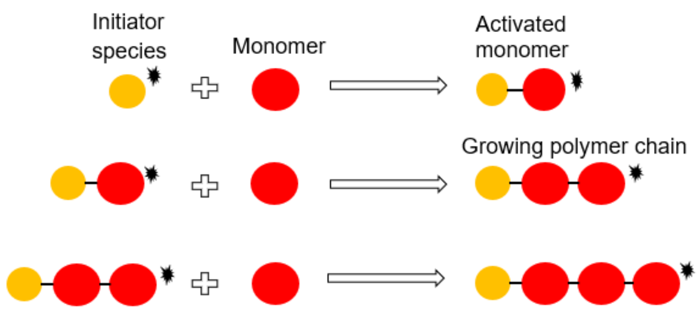

Figure 7. Schematic illustration of the chain-growth polymerisation [25; 29; 30].

3.3.1 Free-radical polymerisation

Polymerisation begins with activating of an initiator species [27]. The species in this polymerisation is a free radical, which can form an electrically charged or a highly polar active group on a monomer [31]. Radical initiators include redox-systems, peroxides and azo-compounds which will initiate the formation of free radical when heat or light are applied [24; 30]. Acrylate or methacrylate monomers are the most typical compounds to polymerase by free-radical mechanism. The polymerisation reaction of acrylates with an initiator and the initiator species R* is presented in Figure 8.

The initiator molecule will decompose providing a free radical, when exposed to heat or light. The activated initiator with the arisen free radical will interact with a monomer forming an initiated monomer with a free radical by breaking the double bond and linking itself to the monomer. The monomer with the arisen free radical is now capable of reacting with another monomer, which is added to the polymer chain by breaking the double bond. The added monomer is now linked to the chain by new bond formation between the activated monomer, and a larger polymer with a free radical is formed. This sequence will continue repeatedly until the termination stage. Polymerisation reaction ends either by combination where two growing polymer chains react with each other forming a bond between them yielding a larger polymer or disproportionation occurs. In disproportionation, a free radical is deactivated by the reaction between two polymers, where a hydrogen atom is transferred between them, and two separate polymers are formed. [24; 27; 30; 31; 32.]

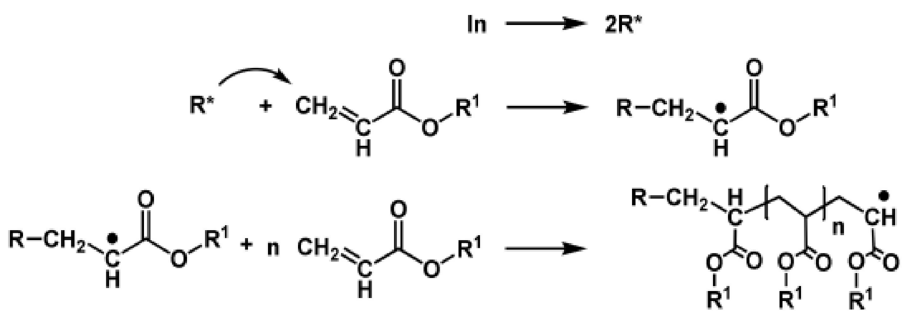

Figure 8. Free-radical polymerisation of acrylates [32].

3.3.2 Ionic polymerisation

Ionic polymerisation is initiated by cations or anions, which means the initiator species in this polymerisation are ions or ion pairs [31; 33]. In cationic polymerisation, the initiator species is a positively charged cation and in the anionic a negatively charged anion. Commonly, occurrence of ionic polymerisations depends on formations of positive or negative ions. [25.]

Cationic initiators are electrophilic substances such as protonic or Lewis acids, carbocations, oxonium ions or metal alkyls; in addition, radiation can be used to initiate the reaction [25; 30]. The initiation step consists of the formation of a cationic initiator species, of the above-mentioned initiators and of the reaction between monomer and the initiator species. The initiator species perform electrophilic attacks on the monomer, where positive charge of the initiator is transferred to the monomer. The monomer is now positively charged, with a linked initiator, and capable of reacting with another monomer. [25, p. 154-156, 151.]

Anionic initiators are nucleophilic substances such as alkali metals, organometallic compounds, Lewis bases or metal amides; in addition, radiation can be used to initiate the reaction [25; 30]. The anionic initiator species is generated from the above-mentioned initiators. The initiator species performs nucleophilic attacks on the monomer, where negative charge of the initiator is transferred to the monomer. The monomer is now negatively charged, with a linked initiator, and capable of reacting with another monomer. [25.]

Polymerisations follow the same propagation step for chain-growth polymerisations. The polymer chain grows by successive additions of monomer units to the reactive centre. The termination of ionic polymerisations is the result of rearrangements in molecule structure or of reactions with other molecules, such as monomer, solvent, and impurities. In anionic polymerisation, the termination step does not occur if contaminants are present or added to the reaction such as water, alcohol, or carbon dioxide. [25.]

3.3.3 Photopolymerisation

Photopolymerisation is a chain-growth polymerisation reaction initiated by photoinitiators, which are free radicals and ions [21; 34]. Initiator monomers have photosensitive properties or reactive sides, which results to generation of initiator species when high-intensity radiation is applied to the process. UV light is typically used as the light source, and other radiation sources such as X-rays, gamma rays, and electron beams can also be implemented. [32; 35, p. 61.] Reaction proceeds in a typical chain reaction mechanism starting with an initiation, followed by propagation and termination stage [34].

Photopolymerisation is the most efficient method to form highly crosslinked polymer network structures, which are very resistant to heat, mechanical stress, moisture, and solvents [21]. The reaction is also rapid, solvent-free, has controllable reaction rates and can be done at room temperature [21; 32]. Photopolymerisation has two main types of reaction mechanisms: free-radical polymerisation of acrylates and unsaturated polyesters, and cationic polymerisation of epoxides and vinyl ethers [21; 35].

Acrylates are highly reactive monomers, which results in high reaction rate when polymerised. One disadvantage is sensitivity to atmospheric oxygen. During polymerisation oxygen inhibition might occur, where some radicals react with oxygen, which in turn limits the initiation and lead to a lower curing degree of polymerised monomers. In cationic reaction, oxygen does not have an impact on initiation stage. However, in the presence of air, chain reactions continue to develop even when the light source is removed. Further curing without the presence of UV light might lead to possibility of higher curing degree or even complete conversion of polymerised monomers. The reaction rate in cationic photopolymerisation is much lower than in the free-radical reaction. [32.]

Curing degree and penetration depth are two factors that should be controlled to have a successful photopolymerisation. The final curing degree after polymerisation affects mechanical properties of the polymer substance. Before the reaction, the curing degree is zero and increases with time, when polymerisation proceeds, due to growth of polymer chains and their crosslinking. Photopolymerisation is an exothermic reaction, which will lead to an increase in reaction temperature. This increase in temperature will impact to the curing degree and is connected to the UV light intensity. Temperature profiles connection to the conversion of acrylate monomers and light intensities are presented in Figure 9. Temperature rises more rapidly when higher UV light intensities are used and lowers slowly, when the maximum value is reached. Temperature stays more stable when lower intensities are used. As can be seen in Figure 9, higher light intensities also lead to faster polymerisation and higher curing degree. The final substance, where high intensities are used, consists of less unreacted molecules. Polymer conversion affects the strength of polymer structure. [32.]

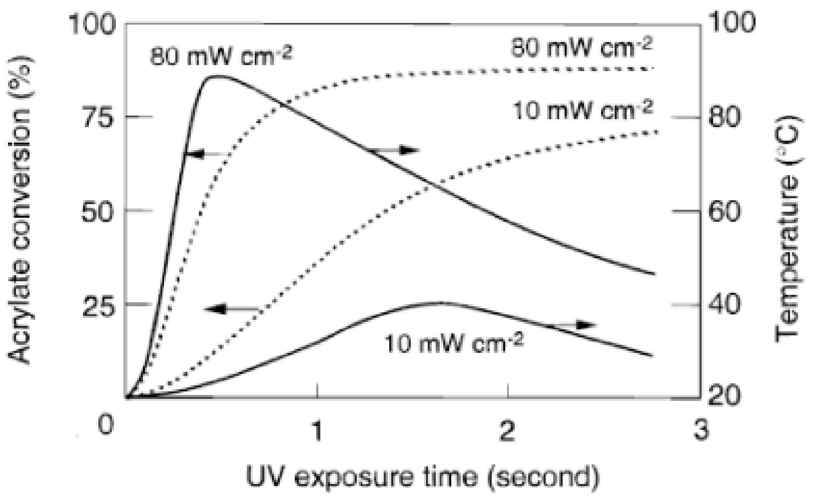

Figure 9. Photopolymerisation of polyurethane-acrylates with different UV light intensities. Temperature profile and exposure time (solid curve). Conversion profile and exposure time (dashed curve). [32.]

Penetration depth limits the possibility of utilizing photopolymerisation. Light intensity decreases along with the penetration depth, which will lead to absorption of light mainly by the photoinitiators on the top layer of the substance. The result of this is a gradient-like generation of an initiator species from the light-exposed side (top side) to bottom of the substance. This will result in lower curing degree in the bottom, due to a lower number of polymerised molecules. The typical thickness of a polymerised layer is 5-200 µm. [32.]

4 Experimental materials and methods

All the tests in this section were executed by using equipment and samples provided by Lumineq Oy and in the facilities of Lumineq and the machine manufacturer Chipital Ltd. The goals of this experiment were to research the capability of the new bonding process to be implemented in selected Lumineq displays. The bonding process was executed utilizing a UV light bonder machine and a conductive UV light cured adhesive. The most important properties of the bonding process are conductivity, adhesion, and mechanical strength of the bond line. The goal was to research suitable bonding parameters and limits from the viewpoint of the above-mentioned properties. Process parameters were optimized following the design of experiment with full factorial design. Test samples were evaluated with visual inspection and connected to power to test functionality. Conductivity of the bond line was evaluated with resistance measurements. In addition, tensile strength and high temperature tests were executed to research reliability and capability of the process.

4.1 Materials and curing devices

Tests were performed on 27 transparent electroluminescent displays. Dimensions of one display in millimetres (mm) is presented in Figure 10. Contact area (pads) of display have thin film ITO pads with a chromium-nickel-vanadium thin layer on top. Every display was bonded using an FPC. The contact area (pads) of FPC are copper with the same pad width and pitch as those of the display’s pad area.

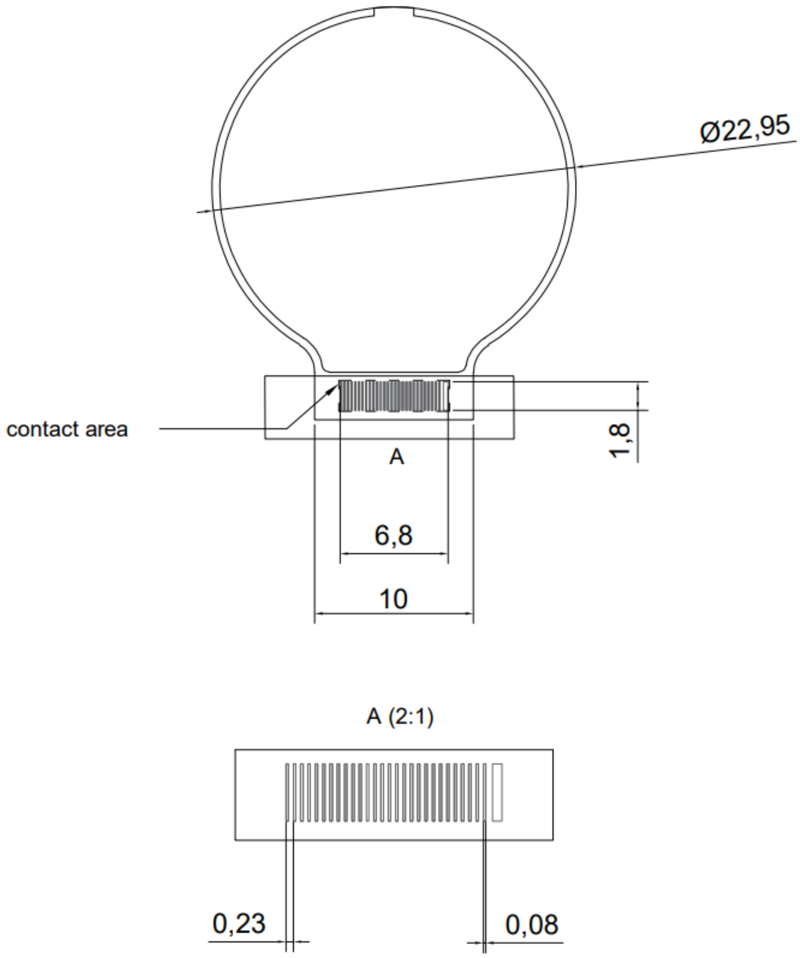

Figure 10. Dimensions of sample display and bonding contact area in millimetres (mm).

Loctite 350 UV light cured adhesive was used as the interconnect material for bonding. Electrical conductivity through the bond line was established by mixing Sekisui Chemical’s gold-coated conductive polymer particles AU-20525 with a diameter of 5.25 µm, with the adhesive. Proportions of the adhesive and particles were measured by a analytical laboratory scale.

Bonding was executed in two steps. The first curing was done at a UV light bonder machine one display at a time. A HOZFR 100 UV light mercury lamp with the power of 2 kW from Hönle was used in the bonder machine. Lamp intensity on different wavelengths is presented in Figure 11. The second and final cure of the adhesive was executed in UV light oven, which has a MHL470/UV-C mercury lamp with power of 450 W from Ushio.

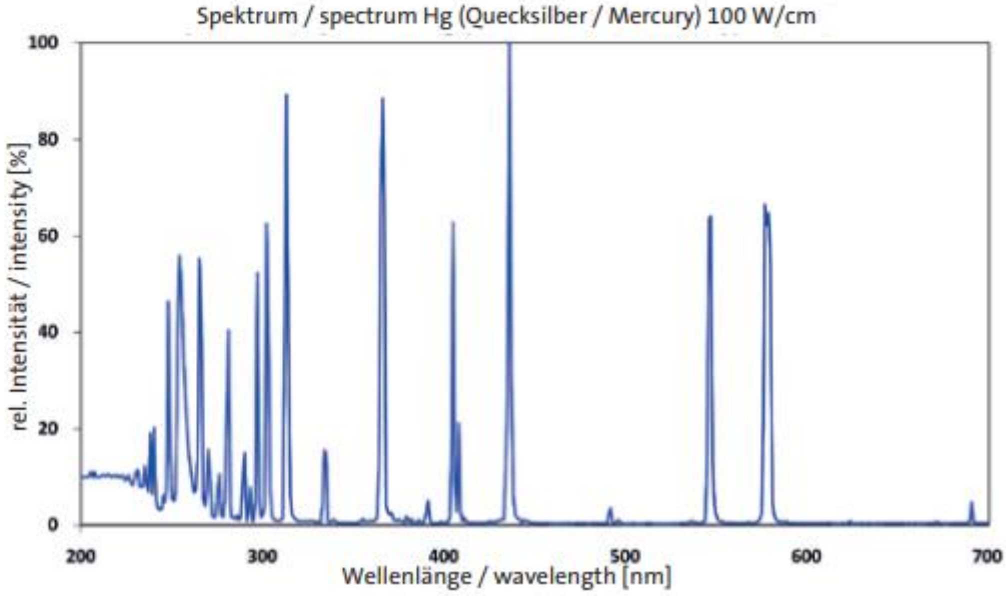

Figure 11. Intensity of the HOZFR 100 UV light mercury lamp used in bonder machine on different wavelengths [36].

4.2 Bonding process

Adhesive preparation

Conductive particles were first weighed using the scale in a mixing cup. Adhesive glue was added on top of the particles and according to desired particle concentration. Compounds were mixed manually with a mixing tool. After mixing, the mixture was heated at 60 ºC in a heating oven for approximately 10 minutes, to lower viscosity. After heating, the mixture was mixed again to achieve more even composition. The mixture was left to cool at room temperature for 5-10 minutes to allow the majority of the air bubbles to exit out of the mixture. The finished adhesive was poured to the dispenser of the UV light bonder machine.

Bonding parameters

Dispenser moves automatically in the direction of the x axis applying the adhesive on top of the pad area of the display. Dispenser pressure, temperature and position were adjustable and set before first bonding. Temperature was set to 35 ºC, to keep viscosity of the adhesive stable. Dispenser pressure was set to 0.25 bar. Adhesive was applied enough to cover the whole pad area of the display, but not overflowing. The position of the dispenser needle was set by adjusting x and y axes coordinates and height of the dispenser. After position settings, the dispenser applies adhesive into the middle of the pad area of the display. The dispenser needle with a diameter of 0.69 mm is set to a couple of millimetres above the display's surface. Bonding pressure and curing time were adjustable.

First cure

The UV light bonder machine has two jigs, one for the display and the other for the FPC. The jigs support the display and FPC with a vacuum on the bottom. There is a prism between the jig of the display and the jig of the FPC, where the pad area of the display sits. The prism allows UV light to penetrate through a bond line. Before bonding, the pad area of the display was cleaned with acetone using cotton buds. The display was placed on the jig with pad side up. FPC was placed on the jig pad area down on top of the display's pad area. After the cleaning and placement, the alignment of the pads of display and FPC was executed with a camera alignment system. The jig of the FPC can be moved manually in the direction of x and y axes, while the display stays in place during the alignment of the pads. The correct alignment is presented in Figure 1. The display was then released for bonding after alignment. The machine will execute bonding automatically where FPC is moved backward, the adhesive is applied to the pad area of the display, and FPC is moved back to the aligned position. After dispensing, the display was moved to under a bonding blade. The used blade was a 2.5 mm wide and has length of a 16 cm.

A simplified illustration of the bonding process in the UV light bonder machine is presented in Figure 12. The bonding blade presses the FPC on the display's contact area at the selected pressure. The force of the applied pressure evens the texture of the adhesive creating a better contact between the conductive particles and the corresponding surfaces of FPC and the display and allows the adhesive to spread creating a protective layer on the contact area. UV light is applied to the process to cure the adhesive. Once cured, UV light is removed, and the blade is released from the bond line.

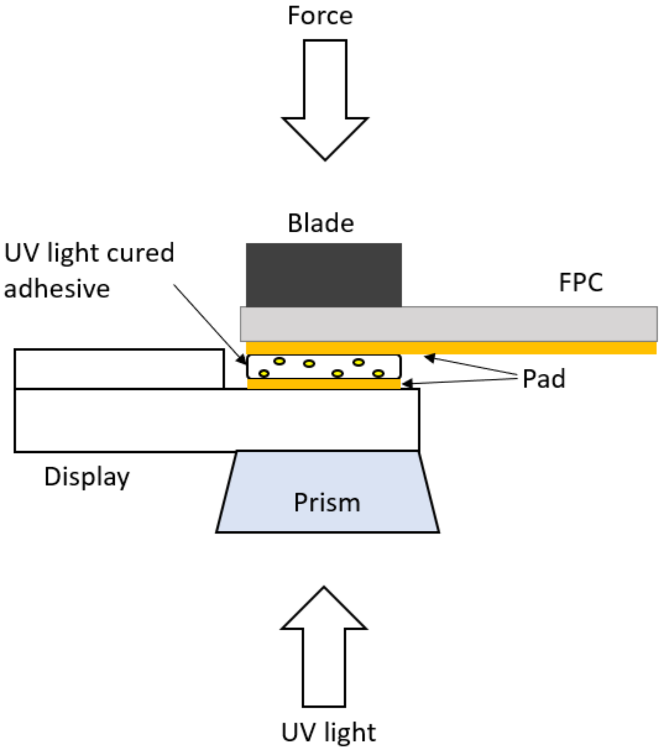

Figure 12. Schematic illustration (side view) of the bonding process in UV light bonder machine with UV light cured adhesive.

Second cure

After the bonding and first cure, the display was moved to a UV light oven for the final cure. The oven has a conveyer belt whose speed can be adjusted. The UV light source is placed on top inside the oven, which means it cures only the one side that is facing the source. Therefore, the display was passed through the oven twice to have a full cure, 60 seconds of UV light exposure on each side.

4.3 Experiment

Design of Experiments (DOE) was executed with 27 tests following a full factorial design 3^3. The bonding process has seven main variables and four of them were kept constant. Selected constants for the DOE were based on previous test results. The constant variables are presented in Table 1.

Table 1. Constant bonding parameters and their values.

Constant variable	**Value**
Second UV light curing time	60 sec/side
Dispenser adhesive temperature	35 ºC
Dispenser pressure	0.25 bar
Dispenser needle size	Ø 0.69 mm

Factor parameters were selected based on their effect on researched properties of the process: conductivity, adhesion, and strength. The factors selected for the DOE were concentration of conductive particles, force and first UV light curing time. DOE consisting of all the parameters for variables of 27 tests are presented in Appendix 1. Every factor has three levels and according to full factorial design 3^3, every level is repeated nine times, enabling a test for every parameter combination. The levels selected for the factors were based on previous test results and presented in Table 2.

Table 2. Factors of the DOE and their levels.

Level	Conductive particle concentration (wt%)	Force (N)	First UV light curing time (sec)
-1	1	20	5
0	2	40	15
1	4	60	25

The tests were executed in three sets following a desired conductive particle concentration (See the sets in Appendix 1). The concentration of the particles was the most difficult factor to adjust during the tests. The adhesive needed to be prepared to the desired concentration and all the tests in this specific concentration were executed before the adhesive exchange. This was repeated until all the tests were completed. Approximately four grams of the adhesive were measured for each set of tests. The conductive particles were measured in the desired weight percent of the total composition of the adhesive.

Some errors occurred during the tests that might have an impact on the results. Also, the position of the dispenser needle might lead to fluctuation in results. The dispenser needle needed to be repositioned each time when the adhesive was changed, including coordinates for x and y axes and the height of the gap between the display and the needle. The adhesive also dripped out of the dispenser while at rest, creating drop on the tip of the needle, which had to be removed before every test. Sample 6 has a larger quantity of adhesive, due to the drop issue. Sample 22 had a longer time of UV light exposure, due the malfunction of the conveyor belt of the UV light oven.

4.4 Test methods

All the bonded samples were visually inspected with microscope analysing the texture of the adhesive, placement, and the deformation of the conductive particles. Functionality of the displays was tested by connecting samples to power and turning them on. All the segments of the samples were lit at the same time as well as one segment at a time to test the full function and make sure each pad had enough conductivity.

A high temperature test was executed in Mean Time Between Failure (MTBF) method to test whether temperature has an impact on the selected factors, and therefore conductivity and adhesion. Samples were strained in three phases with increasing temperature after each phase. Conditions were executed following a standard: Basic environmental testing procedures 60068-2-2 from International Electrotechnical Commission (IEC). Moisture affect was not researched and therefore humidity was kept constant at 40 %. Samples were turned on and connected to the power for 16-hour phases with selected temperatures. The first phase started at room temperature at 22 ºC. The temperature was increased to 40 ºC in the second phase and finally to 85 ºC. After each phase, all the samples were inspected visually with a microscope and lit, turning all the segments on at once and one by one.

The strength of the bond line was tested with a tensile pull test using LR_Plus Series and EZ Series Universal Test Machine from Lloyd Instruments. The test was executed as a peel strength test by pulling the FPC apart from the display in 90-degree angle until the bond line breaks and display and FPC are detached. Schematic illustration of the pull test setup is presented in Figure 13. The machine pulls the FPC at a speed of 3 mm/min, which causes a break in the bond line within 90 seconds. Results are expressed in maximum load values in units of force Newtons (N). The maximum load is reached before the set breaking point of test setup. The load should rise above the load threshold 3 N, and after reaching the maximum load, a breaking point occurs when the load drops by 25% and remain under both values for 1 second.

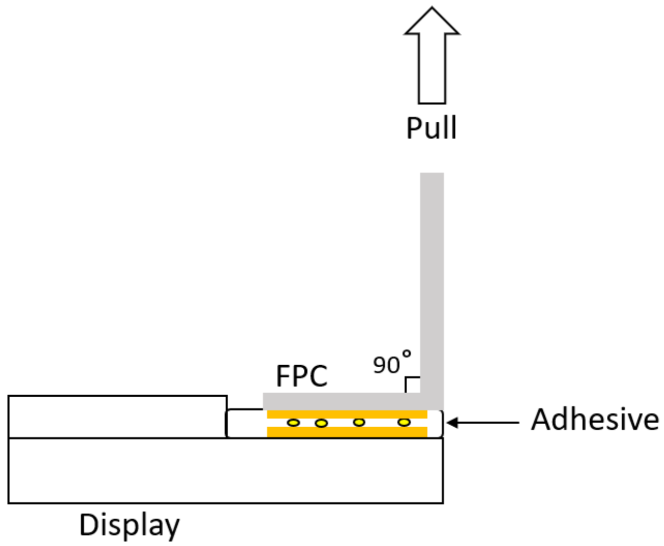

Figure 13. Schematic illustration (side view) of the tensile pull test setup.

Conductivity was examined using resistance measurements with a Dual Display LCR meter model 880 from BK Precision. Additional 27 samples were bonded using the same parameters (Table 1). The thin film structure of the additional samples is a patterned ITO film, which forms an electrical circuit on the display and enables the measurement of resistance on the bond line. Resistance is measured in units of Ohm (Ω) at two points (two pads) at the ends of the FPC. A schematic illustration of resistance measurement is shown in Figure 14. Changes were made to the pressure meter between the original experiment and additional tests, which limits the lowest value of the force to 28 N compared to 20 N used in original experiment. DOE of the additional test with parameter combinations is presented in Appendix 2.

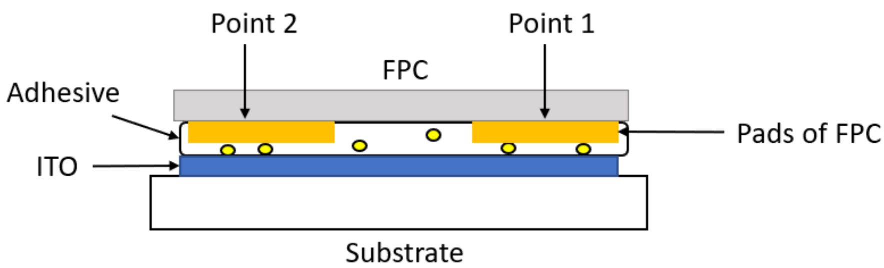

Figure 14. Schematic illustration (cross-section view) of the resistance measurement setup.

5 Results and discussion

5.1 Visual inspection and functionality

Adhesive texture and gold particle placement looked even in all samples when visually inspected. Some air bubbles occurred in the bond line, more on the samples with shortest first curing time of 5 seconds. In addition, some detachment between FPC and display was present in the mentioned samples, as shown in Figure 15. Gold particle deformation could not be inspected visually between pads of the display and FPC due to metallic layers.

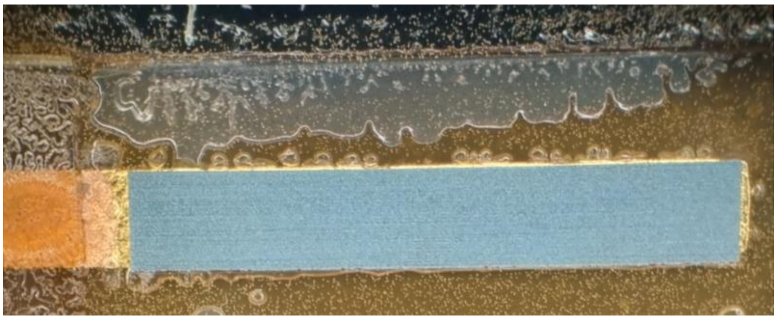

Figure 15. Air bubbles and FPC detachment on the bond line.

All the samples had full function when connected to power. Every segment of the displays turned on and off normally. All the different conductive particle concentrations provided enough conductivity to each pad for full function of the display. Deformation of the particles between pads was visually inspected in additional samples, shown in Figure 16. Particles in the samples with the highest value of used force (60 N) are slightly more crushed than the particles in the samples with the lowest value of used force (20 N and 28 N). Contact surface-area of particles is larger in the samples with higher used force as shown in Figure 16 (right). However, the applied force did not have a major effect on functionality of the displays.

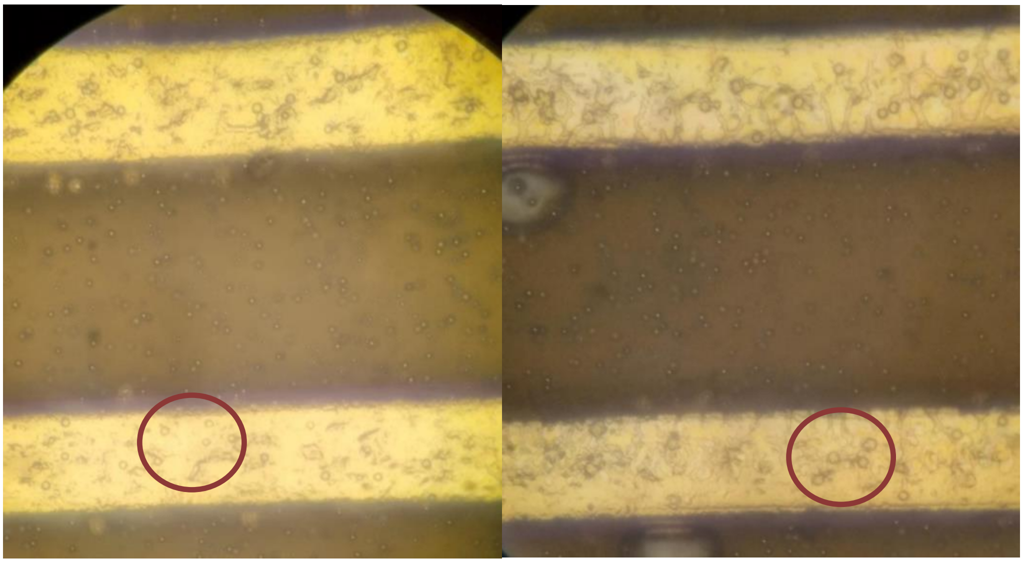

Figure 16. Conductive particle deformation between pads of FPC and display. Particles on the sample with 28 N force used (left) and with 60 N force used (right).

Lastly, samples were turned on in a 16-hour phases in high temperature test starting at the room temperature of 22 ºC. Failures in function or visual changes did not occur after the first phase and inspection. After the second phase at 40 ºC temperature, no new changes were discovered during the inspection. The final inspection was done after the third phase at 85 ºC temperature. All the samples functioned normally. Some detachment in the bond line between FPC and display in a couple of samples was discovered during inspection, but without any clear connection between samples, shown in Figure 17. However, samples were fully functional, which indicates it did not have impact on the electrical contact between pads.

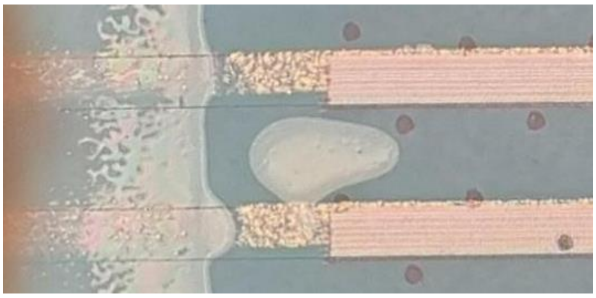

Figure 17. Detachment on the bond line between FPC and Display.

5.2 Design of Experiment (DOE)

Resistance measurements and results from peel strength test were analysed with Minitab data analysis software. The design of experiment was based on three factors (conductive particle concentration, force and first UV light curing time) and three levels for each parameter. Resistance and peel strength test results were added to the software as the responses. Software analyses the impact of a single factor as well as the factor's combined impact on the response (resistance or maximum load) using general factorial regression test with full factorial design 3^3.

The software creates four-in-one residual plots from the results (normal probability plot of residuals, histogram of residuals, residuals versus fitted values and residuals versus order of the data). Residuals indicate how well model fits to data. Residuals in two of the last-mentioned plots in ideal situation should be randomly scattered in both directions positive and negative, without showing a pattern between them.

The impact of each single factor and the factor's combined impact on the resistance and maximum load is presented in a Pareto Chart. The size of the bar represents the magnitude of the impact. Factors with longer bars crossing the reference line (red dashed line) have a significant impact on the response.

5.2.1 Resistance

Resistance measurements of additional samples (see the DOE in Appendix 2) to examine the conductivity of the bond line are presented in Appendix 3. Resistance shows how material resists/reduces the electric flow in an electrical circuit. Resistance measurements allow to research different factors impact on the conductivity. Sample with higher measured resistance reduces the electric flow more, which indicates lower conductivity. Lower resistance value means more electric flow passes through an electrical circuit, which indicates higher conductivity on the sample.

Figure 18 shows the four-in-one residual plots for resistance (normal probability plot of residuals, histogram of residuals, residuals versus fitted values and residuals versus order of the data). Normal probability plot and histogram shows a quite linear line and bell-shaped histogram, which typically indicate to normal probability distribution. Some outlier points can be seen on both ends of the line and histogram, which may have result from the execution of the tests. Tests of the DOE were not executed in randomized order, due to selected factors and testing environment, which could have led to some deviation in the results caused by factors not related to researched elements. Adhesive could not be changed between the tests to proceed execution in a random order. Therefore, tests were executed in sets (Appendix 2) with one adhesive with desired conductive particle concentration at a time. In addition, quality of ITO thin film on the display may vary from sample to sample effecting the resistance results. Residuals are quite randomly scattered in both directions positive and negative in residuals versus fitted values plot, which supports the model. Some pattern is shown at the end of the observation order in residuals versus order of the data plot.

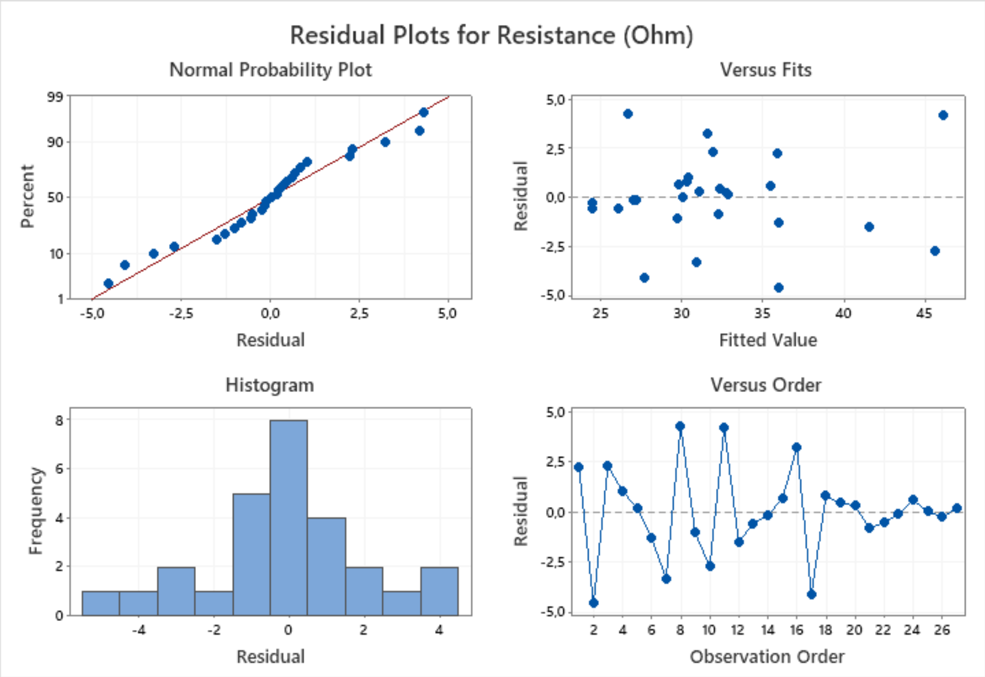

Figure 18. Four-in-one residual plots for resistance. Normal probability plot of residuals (left upper corner), histogram of residuals (left lower corner), residuals versus fitted values (right upper corner), residuals versus order of the data (right lower corner).

The impact of each single factor and the factor's combined impact on the resistance is presented in a Pareto Chart in Figure 19. The size of the bar represents the magnitude of the impact. Factors with longer bars have the largest impact on the response (resistance) and bars crossing the reference line (red dashed line) have a significant impact on the response. Three factors for the DOE were conductive particle concentration (A), Force (B) and UV light curing time (C). As seen in the Figure 19, force (B) has the greatest impact on the resistance. Also, combined impact of particle concentration and Force (AB) is significant.

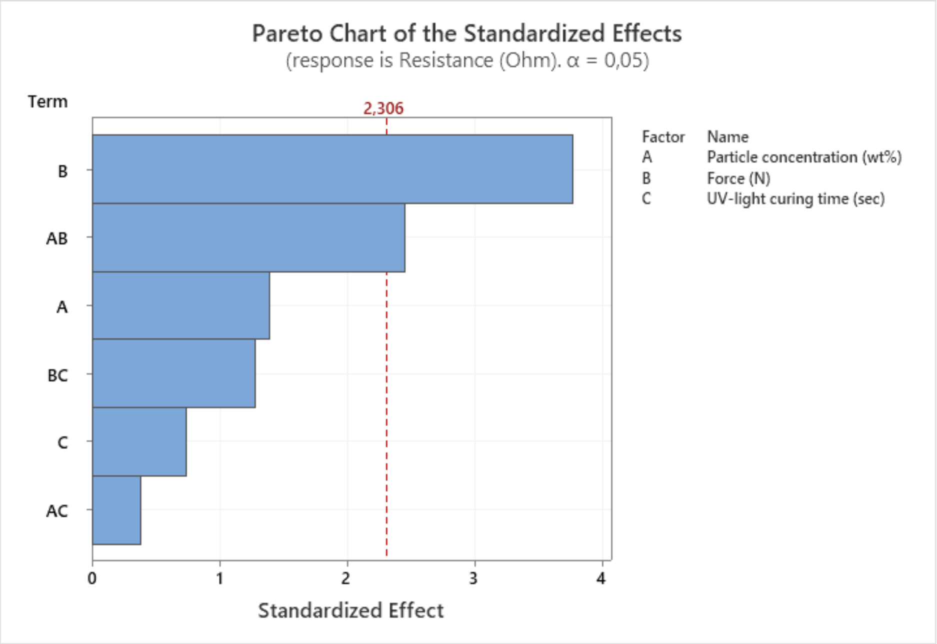

Figure 19. Pareto chart of impact of a single factor and factor's combined impact on the resistance.

The impact of each single factor to resistance is researched more closely using main effects plot for resistance. The effect of each factor in every level is presented graphically in Figure 20. As can be seen, force has the highest impact on resistance, with the longest line between data points of each level (middle). Resistance is highest when using the lowest value of force (28 N) and decreases when higher forces are applied (40 N and 60 N). As discussed in section 2.2.1, applied force deforms the shape of the conductive particles squashing them between the pads of FPC and display. Particles squash more due to higher force, creating a larger surface-area between the pads, as can be seen in Figure 16. This leads to a better conductivity, which shows as a lower resistance. The surface-area of the particle is smaller when the lowest force is used (Figure 16), which shows as a higher resistance, and thus a lower conductivity.

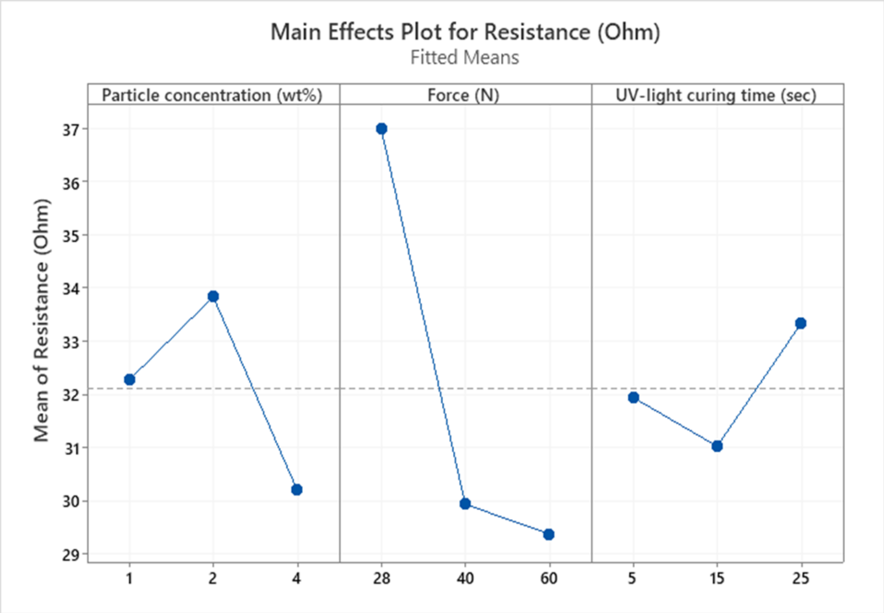

Figure 20. Main effects of particle concentration (left), force (middle), and UV light curing time (right) on resistance.

The impact of two factor's interaction in each level of the resistance is presented graphically in Figure 21. Parallel lines indicate that there is no interaction impact of two factors on the resistance. The more nonparallel the lines are, the greater the magnitude of the interaction. Particle concentration and the force interaction impact on the resistance is shown to be significant as presented in Figure 19. The interaction plot of particle concentration and force (left upper corner) in Figure 21 also shows nonparallel lines. Conductive particle concentration did not have a major impact as a single factor (Figure 19). Decrease in resistance is not significant when particle concentration is increased, as can be seen in Figure 20. However, resistance is higher when smaller quantities of particles are used (1 wt% and 2 wt%) and decreases at highest concentration (4 wt%). Significance of the interaction impact with force may result from multiplying electrical paths between the pads when particle concentration is increased. Therefore, the surface-area increases as well.

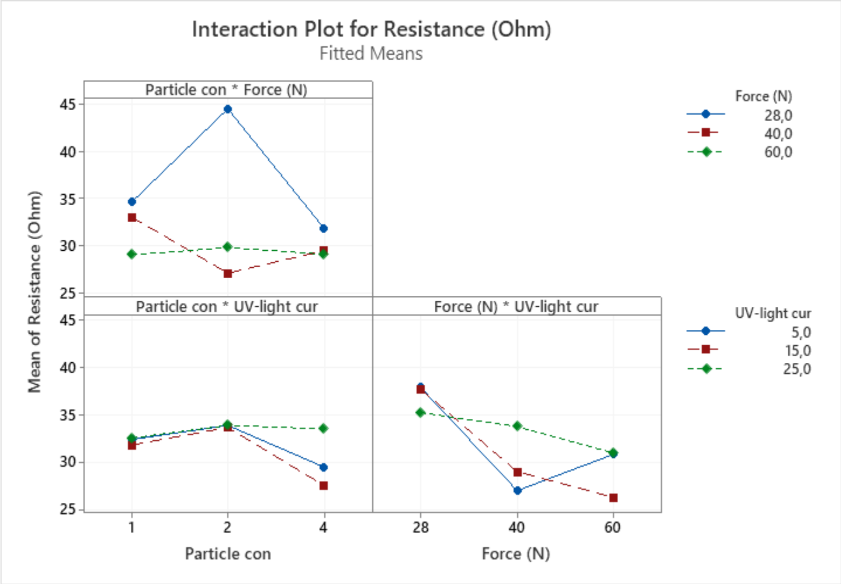

Figure 21. Impact of two factor interactions on resistance. Interactions of force and UV light curing time (right lower corner), particle concentration and UV light curing time (left lower corner) and particle concentration and force (left upper corner).

5.2.2 Adhesion and strength

Adhesion and strength of the bond line of the original samples (see the DOE in Appendix 1) were tested with tensile pull test using a peel strength test. Results in maximum load values are presented in Appendix 4.

Figure 22 shows the four-in-one residual plots for maximum load (normal probability plot of residuals, histogram of residuals, residuals versus fitted values and residuals versus order of the data). Normal probability plot shows quite linear line, typical to normal probability distribution. Some outlier points can be seen in the lower end of the line. Histogram does not show the typical bell-shape to normal probability, which indicates some deviation is present in the data. As covered in the resistance results, tests of the DOE were not executed randomized which could have led to deviation in results caused by factors not related to researched elements. In addition, some variability might have been present in test setup during exchanging the samples. Even though setup was prepared minimizing the variability as much as possible, samples were placed and secured manually. Some issues with the dispenser also occurred as mentioned earlier, dripping of the adhesive and repositioning of the dispenser needle after adhesive change might have had an impact on the quantity and distribution of the adhesive. Also, samples were strained in high temperature test before the strength test, which caused some visual changes in the adhesive (Figure 17). Temperature might have caused a change in the texture of the adhesive. Residuals are quite randomly scattered in both directions positive and negative in residuals versus fitted values plot and no clear pattern is shown in the residuals versus order of the data plot, which supports the model.

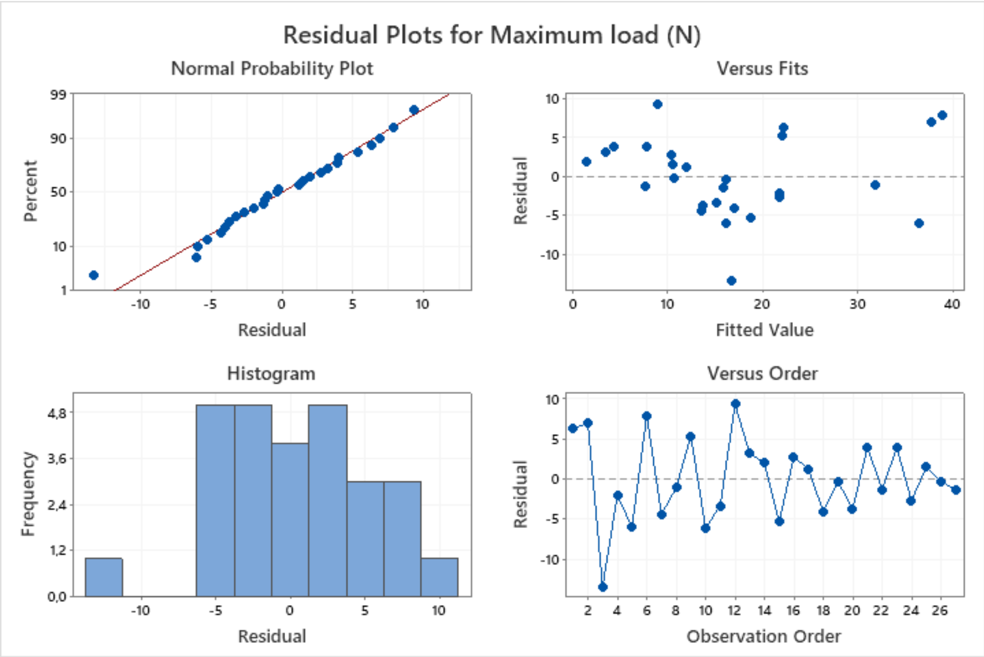

Figure 22. Four-in-one residual plots for maximum load. Normal probability plot of residuals (left upper corner), histogram of residuals (left lower corner), residuals versus fitted values (right upper corner), residuals versus order of the data (right lower corner).

The impact of each single factor and factor's combined impact on the maximum load that bond line can withstand before breaking is presented in a Pareto Chart in Figure 23. The size of the bar represents the magnitude of the impact. Factors with longer bars have the largest impact on the response (maximum load) and bars crossing the reference line (red dashed line) have a significant impact on the response. Three factors for the DOE were conductive particle concentration (A), Force (B) and UV light curing time (C). As seen in the Figure 23, particle concentration (A) has the greatest impact on the strength of the bond line.

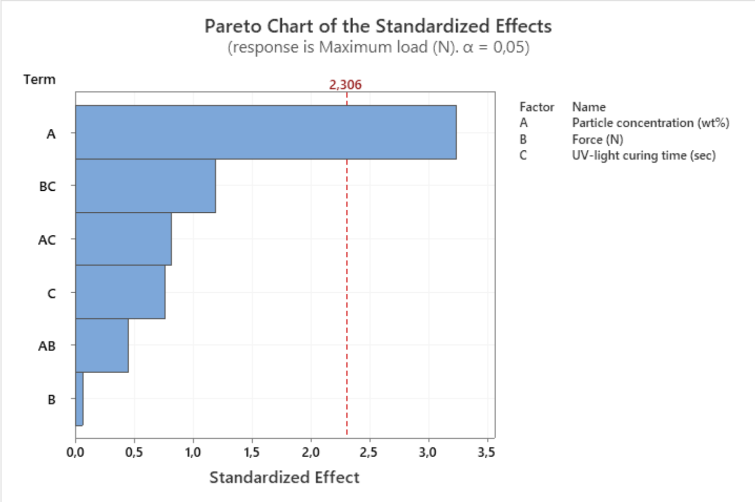

Figure 23. Pareto chart of impact of a single factor and factor's combined impact on the maximum load.

The impact of each single factor on peel strength is researched more closely using a main effects plot for the maximum load. The effect of each factor in every level is presented graphically in Figure 24. As can be seen, the conductive particle concentration has the highest impact on the maximum load, with the longest line between data points of each level (left). The maximum load is highest when using the smallest quantity of particles in the adhesive (1 wt%) and decreases when concentration of particles is increased (2 wt% and 4 wt%). The quantity of conductive particles in the adhesive might have some impact on the texture of the adhesive, which affects the strength of the bond line.

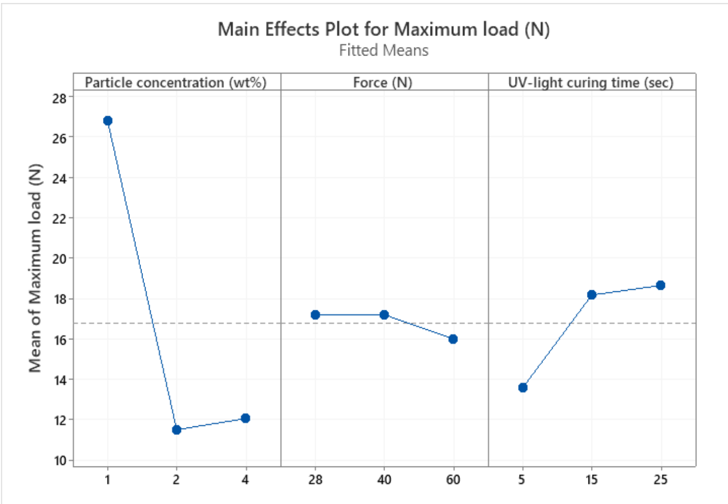

Figure 24. Main effects of particle concentration (left), force (middle) and UV light curing time (right) on maximum load.

Ni XJ and Liang TX [37] conducted a study where UV curing anisotropically conductive adhesive were developed using conductive metallic fillers. Adhesive strength was tested after UV light curing along with same adhesive without the metallic fillers. According to the study, nonconductive adhesive withstood more stress in shear strength test compared to anisotropically conductive adhesive. Added metallic fillers to the UV light cured adhesive can act as terminators to the polymerisation reaction in free-radical photopolymerisation, leading to lower curing degree. The study also mentions that metallic fillers have a lower strength and adhesion than the adhesive itself on the interface of material where adhesive was applied. [37.] As mentioned in section 2.1, electrically conductive adhesives (ECAs) consist of conductive metallic fillers and polymers, which form crosslinked polymer networks after curing. Networks provide adhesion and mechanical strength to the bond line and metallic fillers provide electrical conductivity. In case of anisotropically conductive adhesives, two interfaces are present between the surface and adhesive: interface of polymer crosslinked networks-material and interface of filler-material [37]. Metallic fillers do not provide adhesion on the interface, which may lower strength of the bond line. During the peel strength test breaking occurred in the interface of display and adhesive.

Considering the findings in the mentioned study, particle concentration might have a considerable impact on the strength and adhesion of the bond line. Larger particle concentrations lower the surface-area for interface between polymer networks and material, which might lower the overall strength of the bond line. Concentration of the metallic fillers was not mentioned in the study.

As mentioned in section 2.2.2, curing of UV light cured adhesive requires transparent or clear surface for adhesive to have UV light exposure. Conductive particles have metallic layers, which might impact on the UV light penetration through the adhesive, leading to a lower curing degree of the adhesive and therefore the overall strength and adhesion.

6 Conclusions

The experiment provided important information about the capability of UV light bonding process and behaviour of the researched parameters in the bonding of FPC to an electroluminescence display. Parameters had no major impact on the functionality of the displays. Conductivity remained even after temperature strain and displays were fully functional. The process is feasible, reliable, and scalable based on this initial experiment and research.

High conductivity was achieved with using highest bonding force and conductive particle concentration. Force had the most significant impact on conductivity, followed by the combined impact of interaction of force and particle concentration. Other researched properties were adhesion and strength of the bonded joint. The lowest particle concentration led to higher strength, which designates the conductive particle concentration as the most significant factor on bond line strength. The bonded joint between FPC and the display require mechanical stress to break. Therefore, strength of the joint when using larger concentrations would be enough for this bonding process.

Future experiments should concentrate on determining process limits for the parameters and therefore specify the process window. In addition, more research is needed to get more data about the process behaviour and to optimize researched properties even further. Resistance could be tested using a higher force and increased particle concentration, to see whether they lead to higher conductivity. Achieving higher conductivity would increase reliability of the process and products. It will lead to lower resistance, which prevents generating heat in the pads. On the basis of the results obtained from this experiment, more tests should be done to test the effect of particle concentration along with UV light curing time. Experiment with and without metallic fillers in the adhesive can be performed to further study the impact of the particle concentration on the adhesion of the bond line. Second curing might have affected the impact of first curing time, so overall impact of UV light requires more investigation.

References

1 Ebnesajjad, Sina & Ebnesajjad, Cyrus. 2014. Surface Treatment of Materials for Adhesive Bonding. 2nd ed. USA: Elsevier.

2 Li, Yi; Lu, Daniel & Wong C.P. 2010. Electrical Conductive Adhesives with Nanotechnologies. USA: Springer Science+Business Media.

3 Bevan, Matthew G. & Romenesko, Bruce M. 1999. Modern Electronic Packaging Technology. Johns Hopkins Apl Technical Digest. Vol. 20, No. 1. 1/1999, p. 22. Available from: <https://www.jhuapl.edu/TechDigest/Detail?Journal=J&VolumeID=20&IssueID=1>.

4 Kim, Sun-Chul & Kim, Young-Ho. 2013. Review paper: Flip chip bonding with anisotropic conductive film (ACF) and nonconductive adhesive (NCA). Current Applied Physics. Vol. 13, Suppl. 2. 20/7/2013, p. 14-25. Available from: <https://doi.org/10.1016/j.cap.2013.05.009>.

5 Liu, Johan. 2001. ACA bonding technology for low cost electronics packaging applications – current status and remaining challenges. Soldering and Surface Mount Technology. Vol. 13, No. 3. 1/12/2001, p. 39-57. Available from: <https://doi.org/10.1108/09540910110407397>.

6 Tajau, Rida; Yunus, Nurulhuda Mohd; Salleh, Mek Zah; Ibrahim, Mohammad Izzat; Mahmood, Mohd Hilmi & Salleh Nik Ghazali Nik. 2015. Development of Palm Oil-Based UV-Curable Epoxy Acrylate and Urethane Acrylate Resins For Wood Coating Application. AIP Conference Proceedings. Vol. 1584, No. 1. 17/2/2015, p. 164. Available from: <https://doi.org/10.1063/1.4866125>.

7 Souk, Jun; Morozumi, Shinji; Luo, Fang-Cheng & Bita, Ion. 2018. Flat Panel Display Manufacturing. 1st. ed. John Wiley & Sons Ltd.

8 Morris, James E. & Liu, Johan. 2000. An Internet Course on Conductive Adhesives for Electronics Packaging. 2000 Proceedings. Electronic Components and Technology Conference (Cat. No.00CH37070). 50th. 21-24/5/2000. Available from: <https://ieeexplore.ieee.org/document/853293>.

9 Yi, Myung-Jin & Paik, Kyung-Wook. 1998. Design and Understanding of Anisotropic Conductive Films (ACF's) for LCD Packaging. IEEE Transactions on Components, Packaging, and Manufacturing Technology: Part A. Vol. 21, No. 2. 6/1998, p. 226–234. Available from: <https://ieeexplore.ieee.org/document/705468>.

10 Busek, D. & Mach, P. 2009. Electrical connection network within an electrically conductive adhesive. International Spring Seminar on Electronics Technology. 32nd. 5/2009, p. 1-4. Available from: <https://ieeexplore.ieee.org/document/5276536>.

11 TECHNOLOGY: LUMINEQ Electroluminescent display technology. Internet. Cited 31/20/2022. Available from: <https://www.lumineq.com/technology>.

12 Chen, Xu; Zhang, Jun; Jiao, Chunlei & Liu, Yanmin. 2006. Effects of different bonding parameters on the electrical performance and peeling strengths of ACF interconnection. Microelectronics Reliability. Vol. 46, No. 5-6. 5/2006, p. 774-785. Available from: <https://doi.org/10.1016/j.microrel.2005.07.115>.

13 Gao, Lilan; Gao, Hong & Chen, Xu. 2015. Recent advances in mechanical properties of anisotropic conductive adhesive film for microelectronic packaging. Soldering & Surface Mount Technology. Vol. 27, No. 4. 7/9/2015, p. 164-177. Available from: <https://doi.org/10.1108/SSMT-10-2014-0018>.

14 Chan, Y.C & Luk, D.Y. 2002. Effects of bonding parameters on the reliability performance of anisotropic conductive adhesive interconnects for flip-chip-on-flex packages assembly I. Different bonding temperature. Microelectronics Reliability. Vol. 42, No. 8. 8/2002, p. 1185-1194. Available from: <https://doi.org/10.1016/S0026-2714(02)00079-3>.

15 Chan, Y.C & Luk, D.Y. 2002. Effects of bonding parameters on the reliability performance of anisotropic conductive adhesive interconnects for flip-chip-on-flex packages assembly II. Different bonding pressure. Microelectronics Reliability. Vol. 42, No. 8. 8/2002, p. 1195-1204. Available from: <https://doi.org/10.1016/S0026-2714(02)00089-6>.

16 CIE Standard 017:2020 ILV: 17-21-008. International Lighting Vocabulary, 2nd ed. 2020. Ultraviolet radiation. Austria: International Commission on Illumination.

17 Ryer, Alex. 1998. Light Measurement Handbook. USA: International Light, Inc.

18 Bednarczyk, Paulina; Mozelewska, Karolina & Czech, Zbigniew. 2020. Influence of the UV crosslinking method on the properties of acrylic adhesive. International Journal of Adhesion and Adhesives. Vol. 102, 102652. 10/2020. Available from: <https://doi.org/10.1016/j.ijadhadh.2020.102652>.

19 Bettles, Tim; Schujman, Sandra; Smart, Joseph; Liu, Wayne & Schowalter, Leo. 2007. UV Light Emitting Diodes – Their Applications and Benefits. IUVA News. Vol. 9, No. 2. 1/2007, p. 11. Available from: <https://uvsolutionsmag.com/stories/pdf/archives/090201BettlesEtAlArticle2007.pdf>.

20 Glöckner, Patrick. 2008. Radiation Curing for Coatings and Printing Inks. Germany: Vincentz Network.

21 Decker, Christian. 2001. UV-radiation curing chemistry. Pigment and Resin Technology. Vol. 30, No. 5. 2001, p. 278-286. Available from: <https://doi.org/10.1108/03699420110404593>.

22 Goss, Bob. 2002. Bonding glass and other substrates with UV curing adhesives. International Journal of Adhesion and Adhesives. Vol. 22, No. 5. 20/6/2002, p. 405–408. Available from: <https://doi.org/10.1016/S0143-7496(02)00022-2>.

23 Nee, Andrew Y.C. 2015. Handbook of Manufacturing Engineering and Technology. England: Springer-Verlag.

24 Singh, Jagdamba & Yadav, L.D.S. 2010. Organic Chemistry. Vol. 3. Pragati Bhawan: Pragati Prakashan.

25 Ravve, A. 2012. Principles of Polymer Chemistry. 3rd. ed. USA: Springer Science+Business Media.

26 McNaught, A. D & Wilkinson, A. 1997. Compendium of Chemical Terminology. 2nd ed. Oxford: IUPAC.

27 Heaton, Alan. 1994. The Chemical Industry. 2nd. ed. Dordrecht: Springer Science+Business Media.

28 Stiile, J. K. 1981. Step-Growth Polymerization. Journal of Chemical Education. Vol. 58, 11. 1/11/1981, p. 662-866. Available from: <https://doi.org/10.1021/ed058p862>.

29 Odian, George. 2004. Principles of Polymerization. 4th. ed. USA: John Wiley & Sons.

30 McGrath, James E. 1981. Chain Reaction Polymerization. Journal of Chemical Education. Vol. 58, 11. 1/11/1981, p. 844-861. Available from: <https://doi.org/10.1021/ed058p844>.

31 Szwarc, Michael & Van Beylen, Marcel. 1993. Ionic Polymerization and Living Polymers. England: Springer Science+Business Media.

32 Lang, Margit; Hirner, Stefan; Wiesbrock, Frank & Fuchs, Peter. 2022. A Review on Modeling Cure Kinetics and Mechanisms of Photopolymerization. Polymers 2022. Vol. 10, 2074. 19/5/2022. Available from: <https://doi.org/10.3390/polym14102074>.

33 Luscombe, Christine K; Moad, Graeme; Hiorns, Roger C; Jones, Richard G; Keddie, Daniel J; Matson, John B; Merna, Jan; Nakano,Tamaki; Russell, Gregory T. & Topham, Paul D. 2022. A brief guide to polymerization terminology (IUPAC Technical Report). Pure and Applied Chemistry. Vol. 94, No. 9. 15/8/2022, p. 1079–1084. Available from: <https://doi.org/10.1515/pac-2021-0115>.

34 Miller, L. J; Margerum, J. D. & Rust, J. B. 1968. Imaging by Photopolymerization. Journal of the SMPTE. Vol. 77, No. 11. 11/1968, p. 1177-1184. Available from: <https://ieeexplore.ieee.org/document/7262731>.

35 Gibson, I; Rosen, D. W. & Stucker, B. 2010. Additive Manufacturing Technologies. USA: Springer Science+Business Media.

36 Components and replacement parts: UV lamps/UV bulbs: Productinformation UV-lamps. Internet. Cited 2023 February 7. Available from: <https://www.hoenle.com/products/components-and-replacement-parts/uv-lamps-bulbs>.

37 Liang, TX & Ni, XJ. 2003. Development of UV-curing anisotropically conductive adhesives. Surface Coatings International Part B: Coatings Transactions. Vol. 86, B4. 12/2003, p. 247-328. Available from: <https://link.springer.com/article/10.1007/BF02699501>.

Design of Experiment (DOE)

	Test	Conductive particle concentration	Force	First UV-light curing time
		wt%	N	Sec.
set 1	1	1	20	5
	2	1	20	15
	3	1	20	25
	4	1	40	5
	5	1	40	15
	6	1	40	25
	7	1	60	5
	8	1	60	15
	9	1	60	25
set 2	10	2	20	5
	11	2	20	15
	12	2	20	25
	13	2	40	5
	14	2	40	15
	15	2	40	25
	16	2	60	5
	17	2	60	15
	18	2	60	25
set 3	19	4	20	5
	20	4	20	15
	21	4	20	25
	22	4	40	5
	23	4	40	15
	24	4	40	25
	25	4	60	5
	26	4	60	15
	27	4	60	25

Design of Experiment (DOE) of additional samples

	Test	Conductive particle concentration	Force	First UV-light curing time
		wt%	N	Sec.
set 1	1.2	1	28	5
	2.2	1	28	15
	3.2	1	28	25
	4.2	1	40	5
	5.2	1	40	15
	6.2	1	40	25
	7.2	1	60	5
	8.2	1	60	15
	9.2	1	60	25
set 2	10.2	2	28	5
	11.2	2	28	15
	12.2	2	28	25
	13.2	2	40	5
	14.2	2	40	15
	15.2	2	40	25
	16.2	2	60	5
	17.2	2	60	15
	18.2	2	60	25
set 3	19.2	4	28	5
	20.2	4	28	15
	21.2	4	28	25
	22.2	4	40	5
	23.2	4	40	15
	24.2	4	40	25
	25.2	4	60	5
	26.2	4	60	15
	27.2	4	60	25

Resistance measurement results

Test	Resistance
	Ω
1.2	38,13
2.2	31,49
3.2	34,26
4.2	31,5
5.2	33,05
6.2	34,71
7.2	27,60
8.2	30,96
9.2	28,74
10.2	42,95
11.2	50,35
12.2	40,05
13.2	23,95
14.2	27,06
15.2	30,54
16.2	34,82
17.2	23,65
18.2	31,12
19.2	32,78
20.2	31,43
21.2	31,47
22.2	25,56
23.2	26,94
24.2	36,09
25.2	30,16
26.2	24,28
27.2	33,06

Tensile pull test results

Test	Maximum load
	N
1	28,46
2	44,77
3	3,49
4	19,84
5	30,57
6	46,79
7	9,31
8	30,84
9	27,36
10	10,17
11	11,90
12	18,31
13	6,77
14	3,52
15	13,48
16	13,20
17	13,26
18	12,90
19	15,83
20	9,98
21	11,77
22	6,48
23	8,21
24	19,14
25	12,03
26	10,47
27	14,59